INSTITUTE OF PHYSICS PUBLISHING JOURNAL OF PHYSICS: CONDENSED MATTER

J. Phys.: Condens. Matter **18** (2006) 4371–4379 doi:10.1088/0953-8984/18/17/022

Superlattice induced by electron-beam irradiation in magnetic ferroelectric $BiMnO_3$

Zhenhua Chi[1], Hua Yang[1], Fengying Li[1], Richeng Yu[1], Changqing Jin[1,3], Xiaohui Wang[2], Xiangyun Deng[2] and Longtu Li[2]

[1] Beijing National Laboratory for Condensed Matter Physics, Institute of Physics, Chinese Academy of Sciences, PO Box 603, Beijing 100080, People's Republic of China
[2] State Key Lab of New Ceramics and Fine Processing, Department of Materials Science and Engineering, Tsinghua University, Beijing 100084, People's Republic of China

E-mail: cqjin@aphy.iphy.ac.cn

Received 5 October 2005, in final form 9 February 2006
Published 13 April 2006
Online at stacks.iop.org/JPhysCM/18/4371

Abstract

Single-phased polycrystalline $BiMnO_3$ (hereinafter abbreviated as BMO) ceramic was fabricated via high-pressure solid-state reaction. Microstructure modification of selective grains, signalled by emergence of superlattice diffraction, was scrutinized by means of electron diffraction (ED) combined with high-resolution transmission electron microscopy (HRTEM). It was clearly evidenced that the well established $C2$ monoclinic substructure ($a = 9.53$ Å, $b = 5.61$ Å, $c = 9.85$ Å and $\beta = 110.67°$) of BMO (Atou *et al* 1999 *J. Solid State Chem.* **145** 639) is metastable and prone to be transformed to a new pseudocubic superstructure ($a \approx b \approx c \approx 15.8$ Å and $\alpha \approx \beta \approx \gamma \approx 90°$) (Yang *et al* 2006 *Phys. Rev.* B **73** 024114) when irradiated continuously by an electron beam. Magnetization measurement unveiled a unique ferromagnetic phase transition at 103 K, which corroborated our speculation that as-prepared BMO ceramic is free of polymorphism at ambient conditions.

1. Introduction

The magnetoelectric subsystem of multiferroics [3], also termed the ferroelectromagnet [4], with coexisting ferroelectric and magnetic order parameters has stimulated a great deal of research interest during very recent years [5–7]. Apart from the tremendous application potential based on the mutual control and coupling of polarization and magnetization via the magnetoelectric effect, i.e., the induction of electric polarization by means of magnetic field and vice versa, the fundamental physics behind multiferroics is fascinating. Unfortunately, the number of ferroelectromagnets is dramatically reduced to a very few cases due to the incompatibility between magnetism and ferroelectricity. Through first-principles computation,

[3] Author to whom any correspondence should be addressed.

Hill and co-workers has pointed out that the partially occupied d level which is a prerequisite for the magnetic ground state reduces the tendency of off-centre structural distortion responsible for polar behaviour [8]. Thus, an additional structural driving force must be present to engender the concurrence of ferroelectricity and ferromagnetism. Lone pair chemistry has proven to play a pivotal role in spawning ferroelectricity in prototypical ferroelectric $PbTiO_3$ [9], which exhibits an entirely different polarization mechanism in comparison with the homologous $BaTiO_3$ due to the stereochemistry of $6s^2$ lone pairs on Pb^{2+}. Similarly, the promising candidate ferroelectric $PbVO_3$ with exceptionally gigantic tetragonal distortion has been obtained by high-pressure synthesis [10]. Like Pb^{2+}, Bi^{3+} with $6s^2$ lone pair configuration is the key factor to trigger ferroelectricity in perovskite multiferroics $BiFeO_3$ [4], BMO [4] and double perovskite Bi_2NiMnO_6 [11]. Perovskite BMO can only be synthesized via high pressure to suppress the strong polarizability of $6s^2$ lone pairs on Bi^{3+} and stabilize the highly distorted polar structure. It has been generally recognized that BMO undergoes successive structural phase transitions above room temperature. The first, related to reversible transition between two monoclinic ferroelectric phases, occurs at about 450–500 K [12]. The second, associated with irreversible ferroelectric to paraelectric phase transition, takes place at 750–773 K [4, 12]. Below room temperature, a ferromagnetic transition takes place at about 105 K without any change in crystallographic symmetry. As for its unexpected ferromagnetism, in sharp contrast with the antiferromagnetism in the homologous $LaMnO_3$, the particular ordering of the partially vacant e_g orbital of Mn^{3+} due to lone pairs on Bi^{3+} is of great significance [13]. In short, $6s^2$ electron lone pairs on Bi^{3+} are the determinant for both ferroelectric distortion and exotic ferromagnetism in BMO. To shed further light on the origin of multiferroism, i.e. coexistence of ferroelectricity and ferromagnetism in BMO, precise characterization of microstructure becomes indispensable. Microstructural characteristics of ferromagnetic perovskite BMO have been under debate ever since its birth [14]. It was primitively assigned to be a pseudo-triclinic perovskite with two equal angles and two equal edges ($a = c = 3.935$ Å, $b = 3.989$ Å, $\alpha = \gamma = 91.47°$, $\beta = 90.97°$) and without any superstructure lines being ascertained [15], and later refined to be a monoclinic ($C2$) superstructure (hereinafter denoted as **I**) by means of electron and neutron powder diffraction [1]. The latter model, confirmed by further neutron powder diffraction [13], has acted as a predominantly fundamental model since then. By means of electron diffraction (ED), both Chiba *et al* [16] and Montanari *et al* [17] have suggested the existence of room-temperature polymorphism in BMO independent of the preparative conditions. They ascribed the polymorphism to be an intrinsic feature of BMO quenched from high-pressure and high-temperature synthesis conditions. Very recently, high-temperature polymorphism in BMO was addressed by Montanari *et al* [18]. They concluded that BMO synthesized at high pressure is polyphasic in nature and undergoes successive polymorph transitions upon heating in different atmosphere. However, we attribute the polymorph evolution in our BMO specimen to be the consequence of electron-beam irradiation. To exclude the complication caused by impurity phases, we have optimized the preparative conditions and obtain a single-phased BMO specimen.

2. Experiment

The polycrystalline BMO specimen was fabricated via high-pressure solid state reaction. A stoichiometric mixture of Bi_2O_3 (Alfa Aesar, 99.99%) and Mn_2O_3 (Alfa Aesar, 98%) was finely ground in an agate mortar, mould-pressed and encapsulated with a gold capsule to circumvent contamination from the ambience. The ultimate synthesis was conducted in a cubic-anvil-type high-pressure apparatus by keeping the reagent mixture at 1323 K and 4 GPa for 15 min. Pressure was released slowly after quenching the specimen to room temperature.

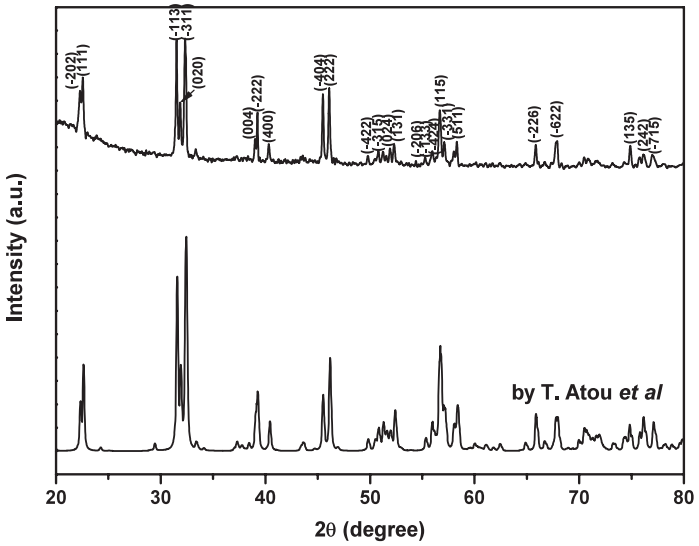

Figure 1. Powder x-ray diffraction pattern of as-prepared $BiMnO_3$ recorded with Cu Kα radiation at room temperature. The Miller indices of all diffraction peaks are labelled.

The powder x-ray diffraction pattern was recorded with Cu Kα radiation ($\lambda = 1.540\,50$ Å) on an M18AHF diffractometer (MAC Science, Japan) to identify the phase constitution of as-prepared BMO ceramic.

The magnetization measurement was carried out in a commercial Mag Lab system. The specimen was cooled in a zero-field mode and measured from 5 to 300 K at an applied field of 0.1 T in the warming run. The hysteresis loop was recorded at 5 K after zero-field cooling.

Selected area electron diffraction (SAED) patterns and high resolution electron microscopy (HREM) images were collected with a Philips Tecnai F20 electron microscope equipped with a field emission gun operating at accelerating voltage of 200 kV, installed at Beijing Laboratory of Electron Microscopy. For TEM observation, the bulk specimen was crushed, milled with alcohol into foil in an agate mortar and suspended on a holey carbon film covered Cu-mesh grid.

3. Results and discussion

Figure 1 exhibits the powder x-ray diffraction pattern of as-prepared BMO ceramic recorded with Cu Kα radiation at room temperature. All the main reflections in the pattern can be indexed on the basis of the $C2$ monoclinic substructure model refined by Atou *et al* [1]. No trace of any kind of impurity phase like $Bi_2O_2CO_3$, Bi-rich or Mn-rich compounds reported in the previous works can be probed in the pattern. In other words, our specimen is excellent for structure characterization in terms of phase purity, which can be attributed to higher reaction temperature and shorter reaction duration compared with the synthesis conditions adopted by Montanari *et al* [17, 18]. The single-phased specimen provides us a good opportunity to reveal both the microstructure feature and the origin of multiferroism in BMO exclusive of the influence of impurities.

SAED patterns of $C2$ monoclinic substructure **I** are displayed in figure 2. It is self-evident that all fundamental perovskite reflections originate from $C2$ monoclinic substructure **I**,

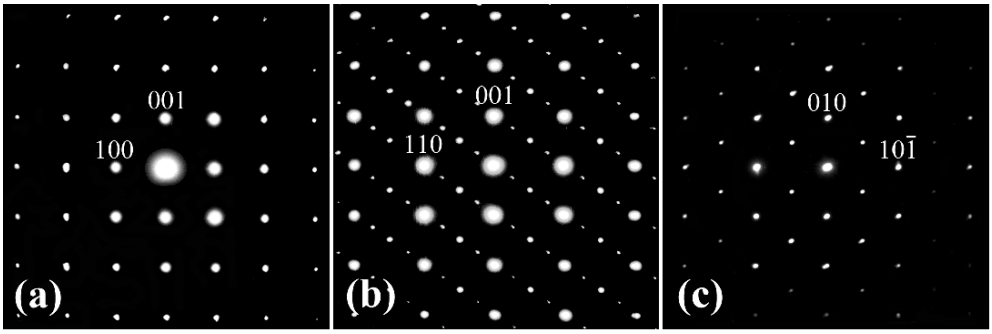

Figure 2. Selected area electron diffraction patterns of $C2$ monoclinically modulated substructure **I** recorded with the incident electron beam along different zone axes of the fundamental perovskite cell. (a) $[010]_p$, (b) $[\bar{1}10]_p$ and (c) $[101]_p$.

whereas Chiba *et al* proposed a monoclinic superstructure ($a = 9.86$ Å, $b = 5.61$ Å, $c = 9.54$ Å, and $\beta = 110.7°$) superimposed on fundamental triclinic substructure ($a = c = 3.94$ Å, $b = 3.99$ Å, $\alpha = \gamma = 91.4°$, $\beta = 90.9°$), i.e., polymorphism, to interpret the complicated ED patterns of their BMO specimen [16]. They found fourfold periodicity in the ED patterns, indicating a larger monoclinic (space group $C2/m$) unit cell with the a- and c-axis lying on the $(10\bar{1})$ plane of the triclinic perovskite lattice and the b-axis elongated along the $[10\bar{1}]$ direction. By ED in combination with HRTEM, Montanari *et al* suggested a triclinic (pseudorhombohedral) superstructure ($a = 13.62$ Å, $b = 13.66$ Å, $c = 13.66$ Å, $\alpha = 110.0°$, $\beta = 108.8°$, $\gamma = 108.8°$) coexisting as a minor phase segregated at the grain surface of the fundamental $C2$ monoclinic substructure [17]. As can be seen in figure 2, no modulation spots associated with new superstructure (hereinafter denoted as **I***) can be discerned in the ED patterns of the as-prepared specimen. All investigated grains exhibit monoclinically modulated substructure **I**, even exposing the same region to electron-beam irradiation for up to 2 h. It should be noted here that all the indices and zone axes in figure 2 refer to the fundamental perovskite cell. In addition, no TEM evidence shows the existence of non-modulated triclinic phase in our specimen.

With the elongation of exposure time to the electron beam, modulation reflections from the new superstructure **I*** emerge and develop, implicating an expansion in unit cell dimensionality with respect to primitive $C2$ monoclinic substructure **I**. As shown in figure 3, the basic reflection spots coupled with commensurate superstructure spots display an apparent higher pseudocubic symmetry, which is consistent with the observation by Montanari *et al* [17]. In particular, the fourfold periodicity along the [111] direction of the fundamental perovskite cell is unambiguous in figure 3(c), similar to the observation by Chiba *et al* [16]. Superstructure **I*** can be imagined to derive from the elongated crystal axes and tilted MnO_6 octahedron of substructure **I**. Taking into account the identical A sites Bi^{3+} and comparable ionic radii between B sites Mn^{3+} and Fe^{3+}, the distortion mode of BMO may be illuminated in the light of sister compound $BiFeO_3$. According to the first-principles study by Neaton *et al* [19], the $R3c$ polar noncentrosymmetric structure of $BiFeO_3$ is distorted from cubic perovskite by two simple pathways: (i) counter-rotation of the adjacent oxygen octahedron around [111]; (ii) relative ionic displacements along [111]. By analogy, in the case of BMO, we can visualize that the Bi^{3+} is displaced relative to the O^{2-} along the [111] direction, accompanied by rotation of the oxygen octahedron around the [111] axis of the cubic perovskite when off-centre distortion occurs. Through first-principles electronic structure calculation, the off-centre distortion of

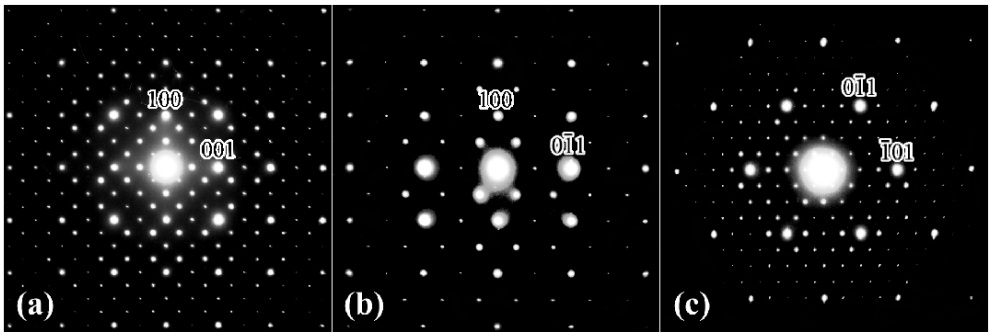

Figure 3. Selected area electron diffraction patterns of pseudocubically modulated superstructure **I*** recorded with the incident electron beam along different zone axes of the fundamental perovskite cell. (a) $[010]_p$, (b) $[011]_p$, (c) $[111]_p$.

BMO from cubic perovskite is ascribed to covalent Bi^{3+}–O^{2-} bonding, i.e., Bi^{3+} 6s and 6p orbital hybridization with the O^{2-} 2p orbital as a result of the lone pair stereochemistry of Bi^{3+} [20, 21]. We can hypothesize that the significant enhancement in symmetry for **I*** in sharp contrast with **I** may be attributed to the suppression of stereochemical activity of Bi^{3+} $6s^2$ lone pairs as a result of electron-beam irradiation. We did track down the gradual evolution of microstructure accompanied by more and more modulated superlattice spots distributing in the background. Eventually, the primitive phase **I** transformed to a completely new modulated phase **I***. As mentioned above, both Chiba *et al* and Montanari *et al* have interpreted that polymorphism is inherent in the as-prepared BMO. In contrast, we propose a novel scenario by introducing the effect of electron-beam irradiation. Whereas Montanari *et al* have excluded the possibility of electron-beam irradiation to induce superstructure **I***, we are definitely convinced of the crucial role of electron-beam irradiation in the appearance of the superlattice in our BMO specimen. It should be pointed out that the as-prepared BMO specimen is oxygen deficient by electron energy loss spectrum (EELS) analysis. The detailed analysis of EELS will be published elsewhere [2]. Under electron-beam irradiation, the oxygen vacancy is inclined to migrate and exhibit to some extent ordered alignment, thus result in subtle distortion of the MnO_6 polyhedron. With increasing irradiation time, the superlattice emerged due to change in the distortion mode of the MnO_6 octahedron. The irradiation-induced superstructure **I*** is stable and does not recover to the primitive substructure **I** even after one week; i.e., the polymorph transition induced by electron-beam irradiation is irreversible.

For further elucidation of the development process, *in situ* high-resolution transmission electron microscopy (HRTEM) imaging of a selected single grain was performed, as is shown in figure 4. It is noteworthy that the transition from **I** to **I*** is not synchronous in different regions. As can be seen in the bottom left corner, the new superstructure **I*** with well defined periodic modulation streaks has been well developed from $C2$ monoclinic structure **I** after considerable exposure time to electron-beam irradiation. On prolonging the irradiation time, the new phase **I*** encroaches upon its adjacent virgin region of primitive phase **I**, as shown in the top right corner. The solid arrows indicate the aggression direction from **I*** to **I**. Detailed analysis of the development process and proposed model are addressed elsewhere [2].

As demonstrated in figure 5, the temperature profile of magnetization of as-prepared BMO at an applied magnetic field of 0.1 T manifested its ferromagnetism with a Curie temperature of 103 K, in excellent agreement with previous reports. Monotanari *et al* has revealed a secondary ferromagnetic transition at 107 K of superstructure phase **I*** in addition to the 99 K transition

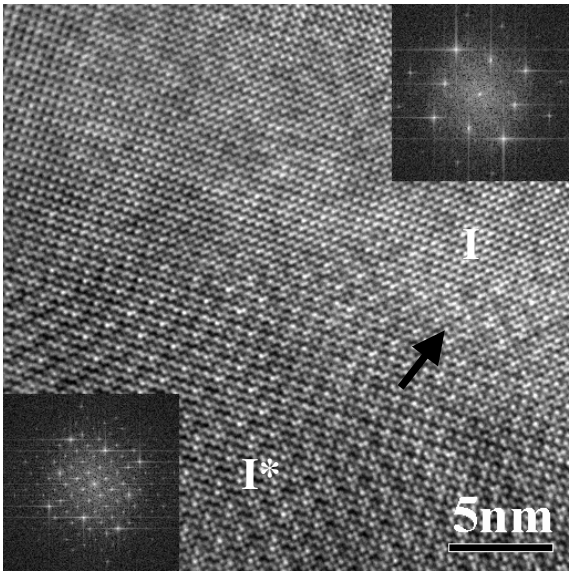

Figure 4. *In situ* high-resolution transmission electron microscopic image of a selected single grain taken along the $[010]_p$ zone axis of the fundamental perovskite cell, indicating the development process from **I** to **I***. The corresponding Fourier transform of the image is shown in the inset.

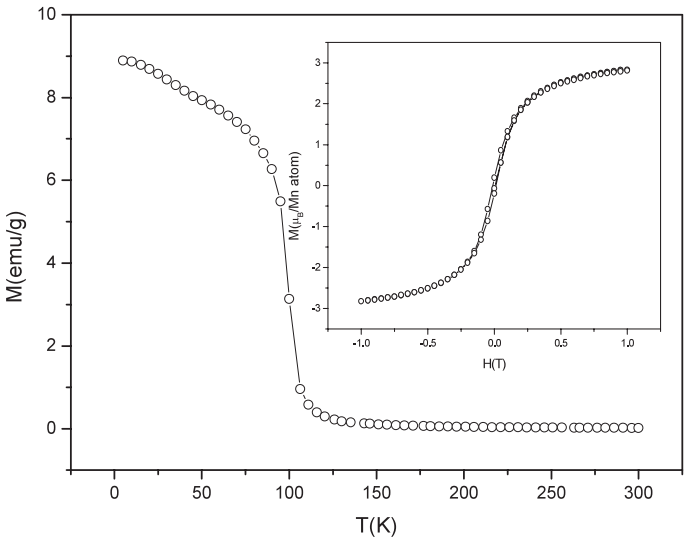

Figure 5. M–T curve of as-prepared $BiMnO_3$ measured from 5 to 300 K at applied magnetic field of 0.1 T after zero-field cooling (ZFC) mode. The inset presents the M–H curve recorded at 5 K.

of monoclinic phase **I** [17]. It is evident in our M–T curve that no trace of a secondary ferromagnetic transition is detectable. This can exclude the presence of polymorph **I***, as is consistent with the ED patterns illustrated in figure 2. The inset in figure 5 presents the M–H hysteresis loop recorded at 5 K. The measured magnetic moment of Mn^{3+} is 2.83 μ_B at 1 T and 5 K, which is smaller than the fully aligned spin value of 4 μ_B for Mn^{3+} ($3d^4$). To account

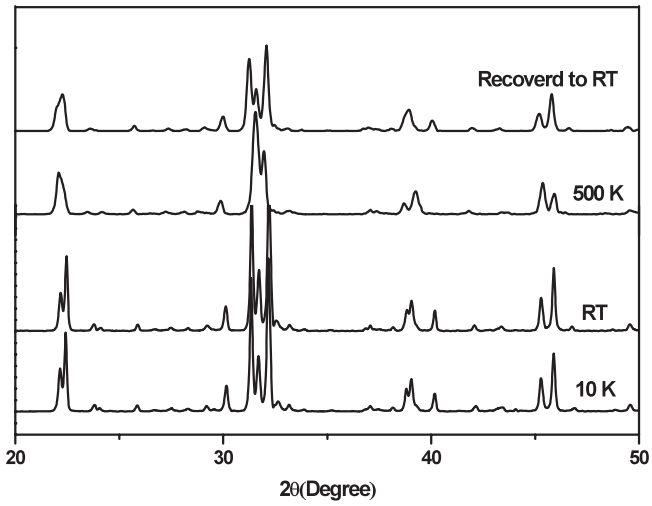

Figure 6. *In situ* variable temperature powder x-ray diffraction pattern of as-prepared $BiMnO_3$.

for this remarkable difference, a distorted Mn–O–Mn super-exchange pathway as a result of cooperation between the Mn^{3+} Jahn–Teller effect and the Bi^{3+} lone pair effect should be taken into consideration. From the hysteresis curve, we can extrapolate the coercive field of 0.02 T and remnant magnetization of 0.2 μ_B at 5 K, indicating a weakly ferromagnetic behaviour of BMO.

The variable temperature powder XRD pattern was recorded by Cu Kα radiation in the temperature range of 10–500 K. It is evident in figure 6 that the crystal structure at 10 K is the same as that at room temperature, indicating no structural phase transition takes place on cooling the polar structure at room temperature through the ferromagnetic Curie temperature down to 10 K, lending support to the belief that ferromagnetism and ferroelectricity coexist in BMO below the ferromagnetic Curie temperature. In contrast, the structure at 500 K is significantly distinct from that at room temperature, reflecting a transition to higher symmetry implicated by the amalgamation of diffraction peaks in the interval between 31° and 33° in 2θ. However, the crystal structure recovered after cooling from 500 K to room temperature; that is to say, the structural phase transition at 500 K is reversible.

The local temperature increment in the specimen caused by electron-beam irradiation during TEM observation is dependent on incident electron energy, current density and thermal conduction behaviour of the specimen [22]. In most cases, it can reach up to the order of magnitude of 10^2 centigrade [23]. This temperature is favourable for an oxygen vacancy to migrate inside the lattice network of perovskite oxides. To test the hypothesis that the superstructure may be a consequence of the heating effect on the specimen by electron-beam irradiation, we simulated the experimental condition of TEM by annealing the specimen at 573 K for 12 h in high vacuum and quenching to room temperature. A comparison between XRD patterns of the BMO specimen pre- and post-anneal is given in figure 7. No salient difference can be tracked in the two patterns. In other words, the structural phase transition at 573 K is reversible. This confirms that the heating effect cannot be the dominant mechanism to induce superstructure in BMO, for the superstructure transition is irreversible, as mentioned above. It goes without saying that the unique factor causing superstructure in our BMO specimen is ascribed to electron-beam irradiation.

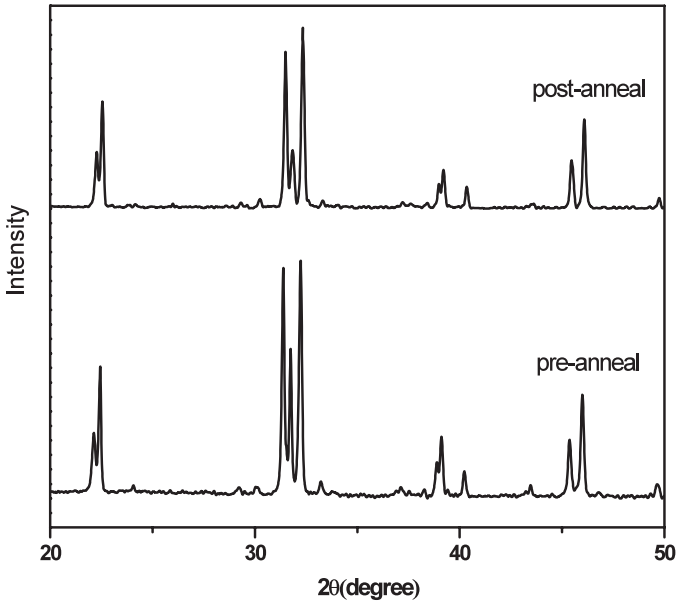

Figure 7. Comparison between x-ray diffraction patterns of as-prepared $BiMnO_3$ before and after annealing at 573 K for 12 h in vacuum.

4. Conclusion

Magnetic ferroelectric BMO ceramic was fabricated by high-pressure solid-state reaction. Multiferroism or ferroelectromagnetism in BMO was assigned to the $C2$ monoclinic substructure **I** due to the single-phase nature of the as-prepared specimen. Pseudocubic superstructure $\mathbf{I}^*$ was induced and developed in metastable monoclinic substructure **I** due to electron-beam irradiation. Room-temperature polymorphism in our BMO specimen was excluded from the viewpoint of both microstructure and magnetization characterization. The significant divergence regarding polymorphism in different BMO specimens may be attributed to different synthesis temperatures, pressures and reaction durations.

Acknowledgments

This work was supported by the Ministry of Science and Technology and NSF of China through the research projects 90401003, 50328102, 2002CB613301, 50321101, 50332020. CQJ is grateful to Professor J S Zhou for inspired discussions.

References

[1] Atou T, Chiba H, Ohoyama K, Yamaguchi Y and Syono Y 1999 *J. Solid State Chem.* **145** 639
[2] Yang H, Chi Z H, Li F Y, Jin C Q and Yu R C 2006 *Phys. Rev.* B **73** 024114
[3] Schmid H 1994 *Ferroelectrics* **162** 317
[4] Smolenskii G A and Chupis I E 1982 *Sov. Phys.—Usp.* **25** 475
[5] Fiebig M, Lottermoser Th, Frohlich D, Goltsev A V and Pisarev R V 2002 *Nature* **419** 818
[6] Kimura T, Goto T, Shintani H, Ishizaka K, Arima T and Tokura Y 2003 *Nature* **426** 55
[7] Lottermoser Th, Lonkai Th, Amann U, Hohlwein D, Ihringer J and Fiebig M 2004 *Nature* **430** 541
[8] Hill N A 2000 *J. Phys. Chem.* B **104** 6694

[9] Cohen R E 1992 *Nature* **358** 136
[10] Belik A A, Azuma M, Saito T, Shimakawa Y and Takano M 2005 *Chem. Mater.* **17** 269
[11] Azuma M, Takata K, Saito T, Ishiwata S, Shimakawa Y and Takano M 2005 *J. Am. Chem. Soc.* **127** 8889
[12] Kimura T, Kawamoto S, Yamada I, Azuma M, Takano M and Tokura Y 2003 *Phys. Rev.* B **67** 180401(R)
[13] Moreira dos santos A and Cheetham A K 2002 *Phys. Rev.* B **66** 064425
[14] Sugawara F, Ihda S, Syono Y and Akimoto S 1965 *J. Phys. Soc. Japan* **20** 1529
[15] Sugawara F, Ihda S, Syono Y and Akimoto S 1968 *J. Phys. Soc. Japan* **25** 1553
[16] Chiba H, Atou T, Faqir H, Kikuchi M, Syono Y, Murakami Y and Shindo D 1998 *Solid State Ion.* **108** 193
[17] Montanari E, Righi L, Calestani G, Migliori A, Gilioli E and Bolzoni F 2005 *Chem. Mater.* **17** 1765
[18] Montanari E, Calestani G, Migliori A, Dapiaggi M, Bolzoni F, Cabassi R and Gilioli E 2005 *Chem. Mater.* **17** 6457
[19] Neaton J B, Ederer C, Waghmare U V, Spaldin N A and Rabe K M 2005 *Phys. Rev.* B **71** 014113
[20] Seshadri R and Hill N A 2001 *Chem. Mater.* **13** 2892
[21] Hill N A and Rabe K M 1999 *Phys. Rev.* B **59** 8759
[22] Gale B and Hale K F 1961 *Br. J. Appl. Phys.* **12** 115
[23] Yokota T, Murayama M and Howe J M 2003 *Phys. Rev. Lett.* **91** 265504